Design Methodology for a SEAREV Wave Energy Converter

Marie Ruellan, Hamid Ben Ahmed, Christophe Josset, Aurélien Babarit, Alain H. Clément, Bernard Multon

Design Methodology for a SEAREV Wave Energy Converter

M. Ruellan, H. Ben Ahmed, B. Multon, C. Josset*, A. Babarit*, A.H. Clément*
SATIE – Antenne de Bretagne de l'ENS de Cachan (UMR CNRS 8029)
* LMF, Ecole Centrale de Nantes (UMR CNRS 6598)

***Abstract* – This article will begin by presenting two power take-off (PTO) technologies for the SEAREV wave energy converter (WEC) followed by the design methodology applied to electromagnetic generator cycles for the "all-electric" solution. We will describe the operating principle associated with the SEAREV WEC before discussing the two conversion technologies intended to transform wave energy into electricity. The types of systems are twofold: hydroelectric and all-electric. The strong coupling between the hydrodynamic, mechanical and electrical phenomena heavily influences the behavior of the recovery (PTO) system and leads to a complex system design that requires a full-scale modeling description.**

A unique design methodology for the all-electric conversion chain has been developed around several distinct control modes, including one featuring power leveling.

***Index Terms* – wave energy conversion - electromagnetic generator - optimization - design methodology**

I. Introduction

According to the World Energy Council (WEC) [1], wave energy constitutes an available and economically-accessible reserve estimated at between 140 and 700 TWh/year, in net terms, i.e. approximately 1% to 5% of the annual worldwide demand for electricity. The recoverable energy could reach as high as 2,000 TWh/year with more efficient conversion systems.

Swells are described as the overlapping of several gradual and monochromatic elementary waves, with all phases being random. Studies have shown that the sea state, i.e. the quantity of energy contained within each of the elementary waves making up a swell, is a slowly-varying non-periodic function. The sea state may be modeled within the frequency space *f* by means of an energy spectrum that depends upon two parameters, i.e.:

- the significant height (peak-to-valley) denoted H_s. This parameter corresponds to the height of the average among the upper third amplitude observations; and
- the peak period T_p, which characterizes the maximum amount of energy within the spectrum.

For an inconsistent swell, the expression in (1) below yields an approximation of its energy potential (in W/m):

$$P = \frac{\rho g^2}{32\pi} . H_s^2 T_p \qquad (1)$$

where ρ is the mass density of water and *g* the gravitational constant.

Table I provides an order of magnitude for the recoverable power vs. swell height H_S and period T_p.

TABLE I
SWELL ENERGY RESOURCE PROFILES

T_p (s)	H_s (m)	P (kW/m)
6	1	2.4
9	2.5	22.5
12	6	173 (hurricane force)

II. Principle behind the SEAREV system

The WEC concept is based on a pendulum set in a closed buoy actuated by the swell through excitation forces [2] (see Fig. 1a). The lever or pendulum executes rotational movements transmitted to an active recovery system (itself coupled to a charge via an electronic power converter), which recovers a portion of its kinetic energy produced. Figure 1b provides a computer graphic of the system featuring hydroelectric conversion [4].

The layout of a PTO that adapts well to the swell characteristics associated with a particular geographic site is to be optimized by incorporating the actual measured swell cycles. Moreover, the design and optimization of such a system in necessitate including the rather strong couplings physically existing between the hydrodynamic, mechanical and control phenomena. In an initial approach, the electromechanical part may be modeled by a simplified recovery function and confined to the recovery braking torque, whose evolution over time has been optimized in the aim of maximizing, for a given set of excitation conditions, electrical energy while minimizing the size of the conversion chain.

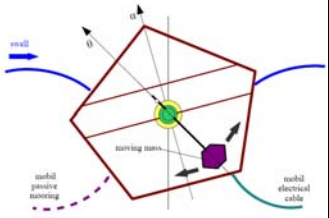

Figure 1a: Schematic diagram of the SEAREV pendular wave energy converter

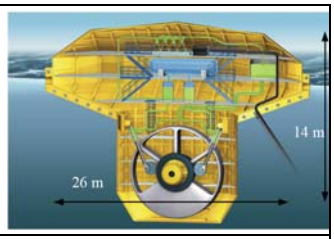

Figure 1b: Computer graphic image of the SEAREV system

The recovered electrical power computation requires determining movements of the coupled device {buoy + pendulum + generator with control}. Hence, a multi-physical hydrodynamic-mechanical-electrical modeling description must be derived.

The general equation to be solved is of the following form:

$$M.\ddot{X} = \sum F_{ext} \quad (2)$$

where M represents the system's inertia matrix and $X = [x_G\ z_G\ \theta\ \alpha]$ is the displacement vector.

F_{ext} is the vector of generalized forces:

$$F_{ext} = F_p + T_R + F_{H+} F_R + F_{ex.} \quad (3)$$

F_p denotes the force being exerted by the pendulum; this force depends on X, $\dot{X}$ and the set of geometric parameters for both the buoy and pendulum.

F_H stands for the hydrostatic force due to buoyancy.

F_R is the so-called radiation force corresponding to the reaction of the {buoy + pendulum} system on the swell.

T_R is the energy recovery torque.

Swell excitation forces F_{ex} are calculated from a set of imposed swell resources for a given overall buoy geometry [3].

In the case of our simplified system set-up, just three swell force components on the buoy warrant attention: the horizontal force F_{ex_X}, vertical force F_{ex_Z}, and *y*-axis moment F_{ex_θ}.

III. Energy Conversion Chain

We will now present the two technological solutions intended to convert mechanical energy from the pendulum excited by the swell into electrical energy.

A. The "hydroelectric" solution

In the specific case of wave energy converters, hydraulic conversion systems are often used given their suitability to wave energy applications, which display the following properties:

- Low speeds and high forces are induced by the waves. In industry, hydraulic systems are commonly used whenever higher forces and smaller motions are required;
- Incident power fluctuates in both time and amplitude. Coupled with a pneumatic storage device, the PTO can smooth incident power fluctuations.

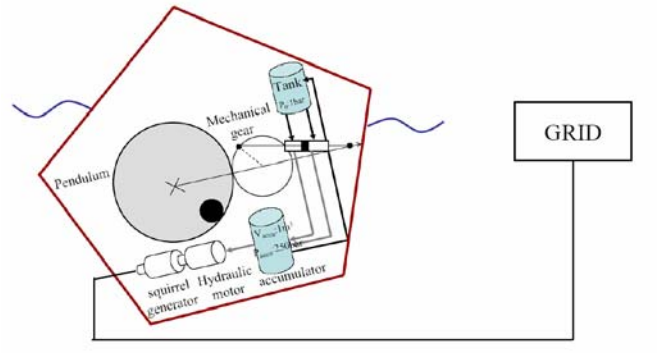

Figure 2: Synopsis of the hydroelectric conversion chain

With a hydraulic solution, the SEAREV PTO is composed of five main elements. First, a mechanical gear is used in order to increase rotational speed while decreasing the input torque. A double-effect linear hydraulic ram, connecting the gear to the floating hull, then transforms the rotation into a high-pressure form; it pumps fluid from the low-pressure tank (atmospheric pressure – 1 bar) to the high pressure accumulator (250 bar), whose volume equals 1 m^3. Energy is stored in this accumulator by means of gas compression. Once enough energy has been stored, the accumulator supplies pressurized fluid at a nominal flow rate to a hydraulic motor coupled to an induction generator, which in turn is directly coupled to the grid. Electricity can then be generated and the fluid is driven back into the tank at low pressure [5].

A sample of the results obtained from this study appear in Table II below.

TABLE II
RESULTS USING THE HYDRAULIC PTO

		Viscous damper	Hydraulic PTO		
T_p (s)	H_s (m)	$E_{extracted}$ (kWh)	$E_{extracted}$ (kWh)	P_0 (bar)	$W_{nominal}$ (kW)
9	1	8	8	30	300
9	3	62	82	150	300
9	5	130	155	190	340

B. The "all-electric" solution

An "all-electric" solution has also been assessed for potential industrial application following an initial electro-hydraulic phase (see Section III.A). The remainder of this article will lay out the design methodology for this solution. The pendulum is damped by an electromagnetic generator driven by an IGBT static converter along with pulse width modulation (2 three-phase bridges, back-to-back on both the machine and network sides), in association with a system that imposes a set of optimized control laws. The generator may be directly coupled to the pendulum (i.e. direct drive) or coupled via a mechanical multiplier (both of these options are currently under study). The research presented herein pertains to the optimal electromagnetic generator design and its static converter solely in the direct drive mode. The multi-physical couplings and swell cycle complexity necessitate developing a specific design optimization methodology that incorporates the control laws.

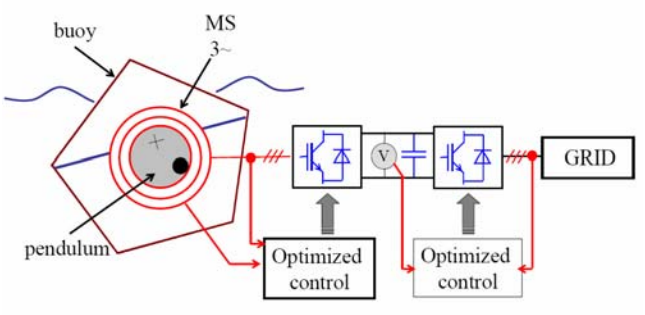

Figure 3: Synopsis of the electro-magneto-mechanical conversion chain

IV. Design Methodology for the "All Electric" Solution

A. A heavily-coupled multi-physical problem

This section will address the design methodology employed for the electro-magneto-mechanical solution.

The system is submitted to fluctuating swells that have previously been characterized. In order to recover the maximum amount of energy, certain elements need to be optimized, namely the hydrodynamic shape of the system, the electromagnetic generator and the control strategy. The coupling between system elements is strong. The buoy has been optimized by the fluid mechanics research team at the Ecole Centrale engineering school in Nantes (western France), while optimization of the electric generator was performed by the SATIE laboratory team working at the ENS de Cachan educational facility. This generator will basically be handled like a device capable of imposing a braking torque $T_R(t)$. Following optimization, it appears that a viscous friction type of torque shape is indeed well adapted:

$$T_R(t) = \beta\dot{\theta}(t) \quad (4)$$

The reaction of this braking torque first on the pendulum, then on both the buoy and swell, has been well taken into account by the general model.

Based on these excitation forces and in accordance with a multi-physical hydrodynamic-mechanical-electrical model, the power and recovered electrical energy are calculated at each point in time over a fixed period ΔT.

Given the coupling indicated above, the choice of control mode exerts a significant influence on overall system behavior as well as on generator design.

The optimization step consists of seeking the law of instantaneous electromagnetic torque variation $T_R(t)$ that maximizes recovered energy and minimizes peak power. The diagram below illustrates this optimization methodology.

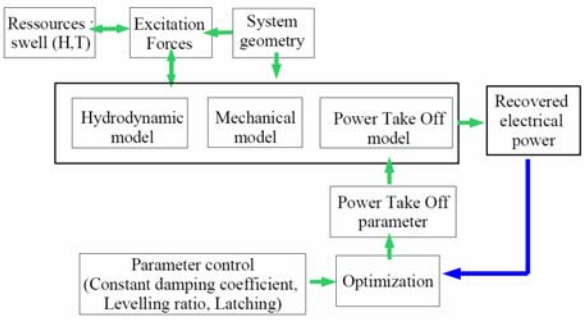

Figure 4: Synopsis of the swell generator design

B. *Control modes*

We have examined three distinct control methods [6]:

- optimization of the viscous damping coefficient β,
- power leveling, and
- latching-based control.

1) *Optimization with constant recovery coefficient β*

We start by imposing a viscous damping type of torque: $T_R(t) = \beta\dot{\theta}(t)$

where β is the viscous damping coefficient, which remains constant over the full cycle period (including during the transient pendular motion start-up phase) yet must still be optimized over the entire cycle. The optimization problem becomes one of seeking the values of β such that the recovered mechanical energy W_e is maximized (see Fig. 5 below).

$$W_e = \int_{\Delta t} \beta[\dot{\theta}(t)]^2 dt \quad (5)$$

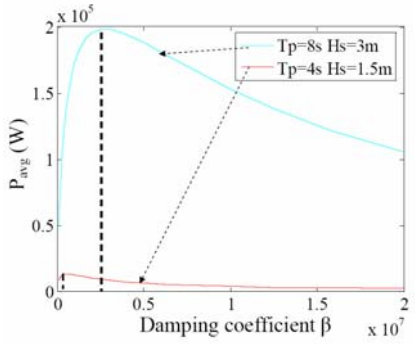

Figure 5: Average power vs. damping coefficient β

Simulations must be run over period cycles $\Delta T >> T_p$ long enough to reach the mechanically-established operating range. We have conducted a sensitivity study of simulation time with respect to the average power calculation.

A minimum simulation time thus proves necessary before the transient state can be neglected. We set a simulation time of 800 sec for the purpose of our simulation runs (see Fig. 6).

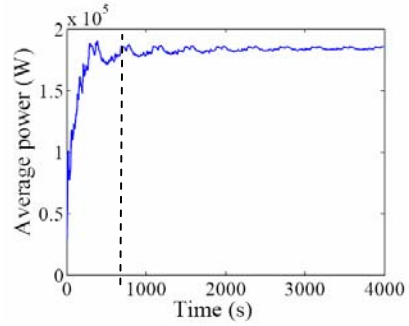

Figure 6: Average power vs. simulation time

Figure 7 displays the fluctuations in recovered power over an 800-sec cycle for a swell with a characteristic height of 3 m and period of 8 sec; this swell will constitute our reference for the remainder of the discussion. The graph shows the very strong variations in instantaneous power, which turn out to be highly penalizing in terms of both system cost and quality of energy produced.

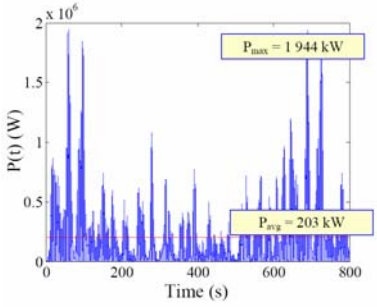

Figure 7: Recovered power with constant β_{opt} over the entire cycle

Simulations were also run on various types of swells. We

tracked the set of points swept in the {Speed, Power} planes (Fig. 8) and {Speed, Torque} planes (Fig. 9) for four types of swells.

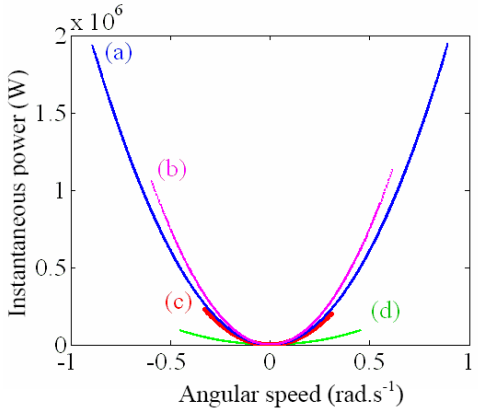

Figure 8: Point cloud of the instantaneous power vs. angular speed for several swells - (a) T_p = 8s, H_s = 3m; (b) T_p = 10s, H_s = 3m; (c) T_p = 5s, H_s = 1m; (d) T_p = 5s, H_s = 2m

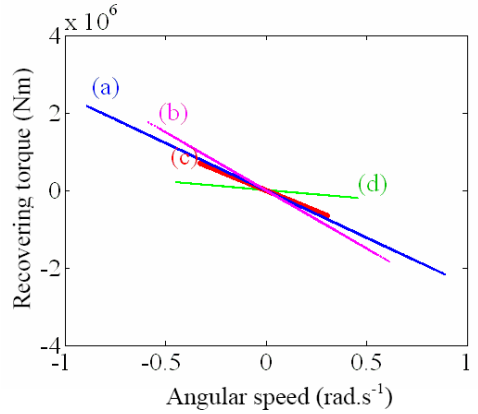

Figure 9: Point cloud of the damping torque vs. angular speed - (a) T_p = 8s, H_s = 3m; (b) T_p = 10s, H_s = 3m; (c) T_p = 5s, H_s = 1m; (d) T_p = 5s, H_s = 2m

The optimal value of recovery coefficient β_{opt} depends on the type of swell acting upon the system and must be adjusted for swell characteristics. We will present below, in the form of a scatter diagram, the average recovered power levels (Fig. 10) along with the corresponding optimal values of recovery coefficient β_{opt} (Fig. 11), for various types of swells.

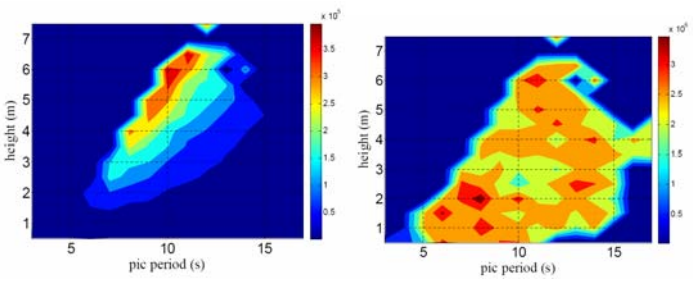

Figure 10: Scatter diagram of average recovered power (W) (left) and optimal recovery damping coefficient β (Nms/rad) (rifgt) with constant β_{opt} over a cycle with constant characteristics

2) Power leveling

The sizable fluctuations in recovered power cause the electric conversion system to be oversized. A leveling of the converted power would therefore serve to better optimize the economic return.

This leveling is obtained in the present case by means of modifying (reducing) the value of the recovery damping coefficient β. For those phases in which the power lies below the imposed leveling power, the value of β is held at an optimized constant, in the aim of maximizing average power over the entire cycle (as is characteristic of constant swells). For those phases in which the power generated is greater than the leveling power, the coefficient β varies temporally such that the power generated remains constant and equal to the leveling power (i.e. generator operating at constant power).

We define the leveling power as $P_{lev} = \alpha\ P_{max.\ before\ leveling.}$ α is the leveling ratio.

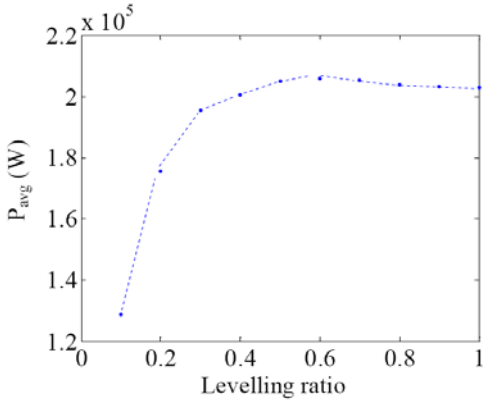

Figure 11: Recovered power vs. leveling power α

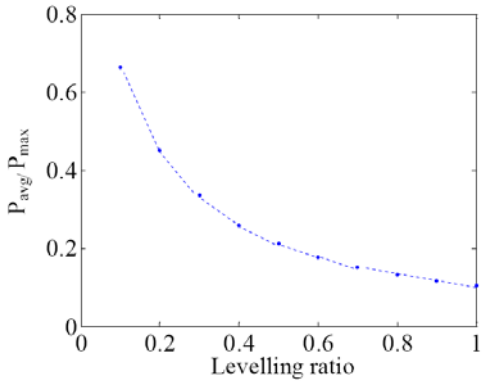

Figure 12: Average power-to-maximum power ratio vs. leveling power α

Such a control has enabled recovering a certain amount of average power while limiting the average power-to-peak power ratio (see Fig. 12). This power recovery is indeed characteristic of the power electronics design. The generator is not directly related to the peak power and undergoes a separate optimization procedure.

We show (fig. 13-14) in both the {Speed, Power} planes and {Speed, Torque} planes the set of points swept during a single swell cycle and for various leveling ratios α on the reference swell.

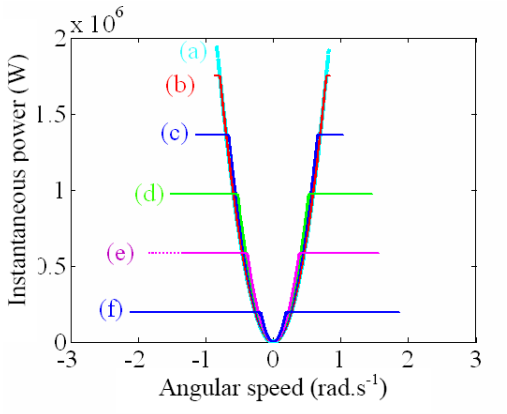

Figure 13: Point cloud of the instantaneous power vs. angular speed for several power leveling ratios - (a: α=1), (b: α=0.9), (c: α=0.7), (d: α=0.5), (e: α=0.3), (f: α=0.1)

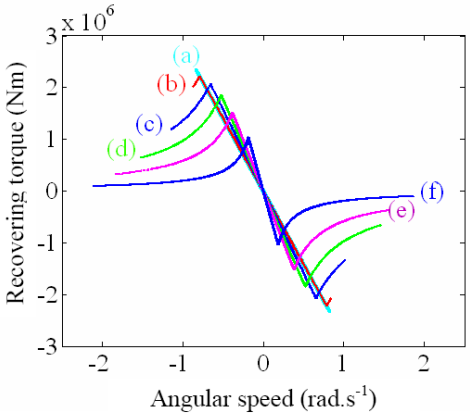

Figure 14: Point cloud of the instantaneous torque vs. angular speed for several power leveling ratios - (a: α=1), (b: α=0.9), (c: α=0.7), (d: α=0.5), (e: α=0.3), (f: α=0.1)

Figure 15 depicts an instantaneous recording of the power for a leveling ratio α of 30%, obtained for the reference swell.

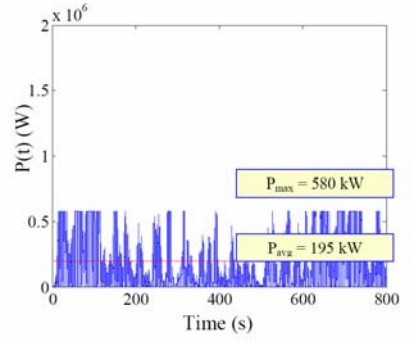

Figure 15: Recovered power after power leveling (30% ratio)

3) *Latching [7]*

Latching control consists of locking (latching) the motion of the body at the instant when its velocity vanishes, while waiting for the wave force to have reached the optimal phase to release the body. The body then starts moving from this initial position to the next vanishing velocity position, where it is once again latched, and so forth and so on. Instead of being a smooth, continuous function, the body position is a succession of transient motion ramps separated by resting stages. Action upon the system is therefore binary: either the body is latched, or it is free to move.

Figure 16 displays the instantaneous power for the reference swell.

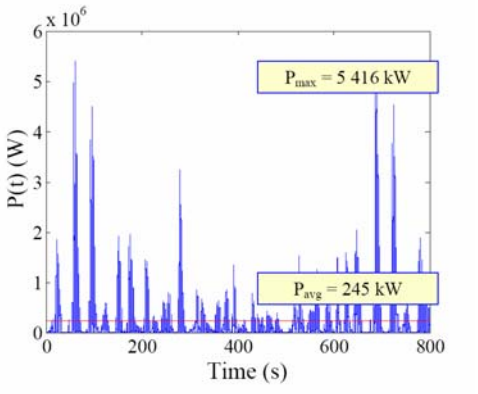

Figure 16: Recovered power with latching control

4) *Electromagnetic generator*

We have sought to perform a preliminary design of the electromagnetic generator on the basis of results obtained from a given swell cycle (i.e. our reference cycle) and with the various types of control already presented.

We conducted this design study on a classical synchronous machine structure featuring surface magnets and a radial field. The study does not allow determining the optimal machine, yet has yielded an applicable methodology [8].

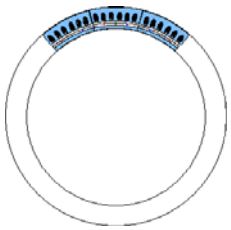

Figure 17: Generator architecture - A synchronous machine with radial flux and mounted surface magnets (only 3 pole pairs shown)

The goal herein is to determine the set of optimal geometric characteristics for the synchronous generator that enable minimizing, from a Pareto perspective, two conflicting objectives: total losses, and the mass of active parts. This search is carried out by focusing on the torque $T_R(t)$ and rotational speed $\Omega(t)$ obtained during the previous system optimization steps over a given operating cycle. In what follows, we will focus solely on the direct-drive solution. Total mass constitutes one criterion among others, as the cost of raw materials could be used similarly in weighting materials by their specific cost instead of their mass density. The design outcome for a swell with a characteristic height of 3 m and period of 8 sec (i.e. the reference swell) is shown in Figure 18. Depending on the site where the swell generator is located, these characteristics might not necessarily be the most severe, but merely serve as an example.

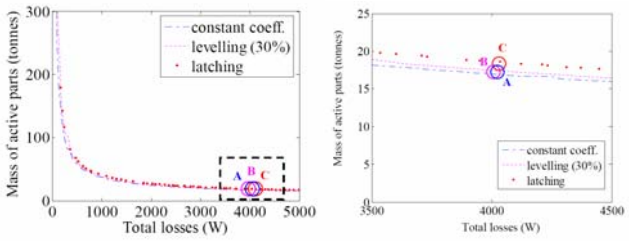

Figure 18: Optimization of the three control modes in direct drive

We are then in a position to compare dimensions of machines with the same 4-kW losses for all three control modes [6].

TABLE 2: OPTIMIZATION RESULTS IN DIRECT DRIVE

	A_1(--)	B_1(--)	C_1(o)
Total active mass (kT)	17	17.4	18.6
Magnet mass (kT)	7.4	7	7
Active volume (m^3)	2.0	2	2.2
External radius (m)	4.3	4	4.4
Length (m)	0.5	0.5	0.5
Number of poles (p)	471	491	497
$<P_j+P_{mg}>$ (kW)	3.9	4	4

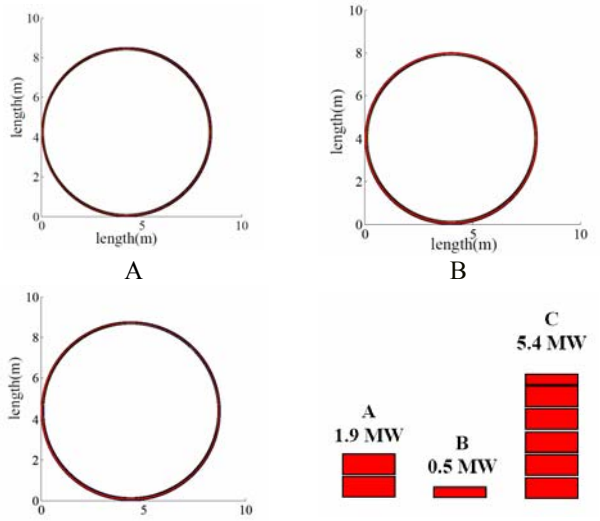

Figure 19: Optimal geometry when employing the various control strategies (A: constant β; B: power leveling; C: latching)

It should be remarked that the generator design for this particular swell is only minimally affected by the choice of control mode. Latching proves to be slightly less favorable. The discrepancy is especially noteworthy on peak power and thus on the cost associated with the static converter.

CONCLUSION

This article presented first the wave energy converter SEAREV.

A design methodology for the "all-electric" solution adapetd to the SEAREV was then offered. Three control modes were studied, specifically one with a constant viscous damping over the swell cycle with a given set of characteristics and power leveling. This particular mode strikes a better economic compromise in designing the entire power conversion chain. Moreover, this control method seems quite straightforward to implement under real world conditions, since sea state characteristics do not in reality change abruptly, and adjusting damping based on a direct evaluation of the sea state can be easily conceived. Optimization results on the peak power design (high levels for the power electronic converter) and in terms of electromagnetic generator mass, with a very large number of poles, were compared across the various control modes. The viscous damping and leveling control therefore appear to be the most promising, although considerable work still needs to be carried out. Power leveling actually requires a field-weakening operating range, and the autopilot angle parameter is to be included in the optimization approach. The incorporation of all system execution constraints will moreover make it possible to determine which electromagnetic conversion structures and electromechanical architecture work best for optimal lever integration. The design methodology described in this article can thus be reused with the specific design models of the selected structure.

Two PTO technologies have been presented: hydroelectric and the "all-electric". For now, it is difficult to compare the two solutions objectively without any real system optimization.

REFERENCES

[1] T. THORPE, "Wave Energy", Chap. 15 of 2004 Survey of Energy Resources, World Energy Council, 2004, pp. 401-417.

[2] A.H. CLEMENT *et al.*, French patent, "Autonomous electrical system for wave energy conversion". In French « Système Electrique Autonome de Récupération de l'Energie des Vagues », 2004.

[3] B. MOLIN "Hydrodynamic of offshore structures" *in French* Editions TECHNIP, Paris, 2002.

[4] Computer graphic image created by Michel Saemann for « Science et Vie Junior », July 2006.

[5] C. JOSSET, A. BABARIT, A.H. CLEMENT, "A Wave-to-Wire model of the SEAREV Wave Energy Converter", Journal of Engineering for the Maritime Environment, accepted for publication in Nov. '06.

[6] M. RUELLAN, H. BEN AHMED, B. MULTON, A BABARIT, A.H. CLEMENT, "Control influence on electromagnetic generator pre-design for wave energy converter". ICEM 2006, Chania, CD-ROM Proc., Sept. 2-5, 2006, 7 p.

[7] K. BUDAL, J. FALNES, "Interacting point absorbers with controlled motion, in Power from Sea Waves". BM Count: Academic Press; 1980.

[8] J. REGNIER, B. SARENI, X. ROBOAM, S. ASTIER "Optimal design of electrical engineering systems using Pareto Genetic Algorithms", 10th European Conference on Power Electronics and Applications, Toulouse, 2003.